January 2006

Diatom paleolimnological record of Holocene climatic and environmental change in the Altai Mountains, Siberia

Karlyn S. Westover
University of Nebraska-Lincoln

Sherilyn C. Fritz
University of Nebraska-Lincoln, sfritz2@unl.edu

Tatyana A. Blyakharchuk
Tomsk State University, Lenina 36, 634050, Tomsk, Russia

Herbert E. Wright
Limnological Research Center, University of Minnesota, 220 Pillsbury Hall, Minneapolis, MN

Published in *Journal of Paleolimnology* 35 (2006), pp. 519–541; doi 10.1007/s10933-005-3241-3

Submitted January 15, 2005; revised and accepted September 12, 2005

Diatom paleolimnological record of Holocene climatic and environmental change in the Altai Mountains, Siberia

Karlyn S. Westover[1,*], Sherilyn C. Fritz[1,2], Tatyana A. Blyakharchuk[3,4], and Herbert E. Wright[5]

[1] Department of Geosciences, University of Nebraska–Lincoln, 214 Bessey Hall, Lincoln, NE 68588-0340, USA
[2] Department of Biological Sciences, University of Nebraska–Lincoln, Lincoln, NE, 68588-0118, USA
[3] Tomsk State University, Lenina 36, 634050, Tomsk, Russia
[4] Institute for Monitoring of Climatic and Ecological Systems, 10/3, Akademichesky Ave., 634055, Tomsk, Russia
[5] Limnological Research Center, University of Minnesota, 220 Pillsbury Hall, Minneapolis, MN 55455-0219, USA
* Corresponding author, email: coyote@unlserve.unl.edu

Abstract
The sedimentary diatom records of three shallow lakes in the Altai Mountains, southern Siberia, were examined to assess the nature and timing of Holocene environmental changes. Few paleoenvironmental records, especially reconstructions not based on pollen, have been reported from this region. The lakes differ in elevation, annual precipitation, and catchment vegetation. Diatom assemblages in all lakes were dominated for the entire period of record by small benthic species of *Pseudostaurosira* Williams & Round, *Staurosira* Ehrenberg, and *Staurosirella* Williams & Round. Planktonic taxa only occur in very low abundances (<5%). The most diverse diatom flora was found in Dzhangyskol, which is situated at the lowest elevation within a forested catchment. A lack of detailed information on the ecological preferences of the dominant taxa and the complexity of environmental drivers make direct interpretation of the diatom record difficult. However, other proxies suggest that dramatic shifts in dominance between *Staurosira elliptica* and *Staurosirella pinnata* in Grusha Ozero reflect millennial-scale variability in climate. Together, chironomids and diatoms provide evidence of a cooling possibly correlative to the Younger Dryas Stade and subsequent early-Holocene warming consistent with pollen evidence of afforestation, which also is likely linked to increased humidity. By 6,000 cal year BP, the transition to a cooler, more continental climate had begun. The diatom record of Akkol shows significantly less variation in diatom community composition, but biogenic silica accumulation rates, a proxy for diatom productivity, appear to reflect climatic variability driven by insolation trends over the past 8,000 years. Long-term variability in Dzhangyskol is not clearly linked to climate.

Keywords: Altai Mountains, biogenic silica, diatoms, Holocene, insolation trends, paleoclimate, Siberia

Introduction

Mountain regions, as a consequence of steep gradients and climatic heterogeneity, are characterized by high ecosystem diversity. As the headwaters for many major rivers, mountains are also a central feature of the global hydrological cycle as well as a crucial source of environmental water for many human populations. Thus, understanding the history and impacts of climate change in mountain regions is es-

pecially critical. Furthermore, many high-elevation sites have experienced recent warming exceeding hemispheric or global averages (Beniston et al. 1997) and may be particularly vulnerable to future climatic changes. Among the regions whose climatic history is poorly known are the southern mountain ranges of Siberia. The Altai Mountains stretch 1900 km along the shared borders of Russia (Siberia), Kazakhstan, China, and Mongolia. They are among the highest in Siberia and form the headwaters of the Ob and Yenisei rivers and of the interior Great Lakes Basin of northwest Mongolia.

The Altai Mountains serve as the locus for the annual development of the Siberian Anticyclone, a central feature of Northern Hemisphere circulation. Zonal flow into the continental interior is blocked during the winter by the Siberian Anticyclone, which is responsible for the calm, cold, and dry winters characteristic of continental Siberia and Mongolia. Periodic additions of arctic anticyclones during winter result in spatial and temporal variability in the strength of the High (Lydolph 1977). Intense heating of the land surface during the summer results in diffuse low pressures over much of the continent, favorable for the penetration of maritime air masses into the interior. Consequently, in the summer, the continental interior experiences a pronounced precipitation maximum. The Altai are characterized by short, cool summers, with a growing season ranging from 160 days in the foothills to 60 days at high elevations (Borisov 1965).

In this paper, we reconstruct the diatom stratigraphies for three lakes in the Altai Mountains. We compare the diatom records with pollen and chironomid data from the same lakes to infer the paleoenvironmental history of this poorly documented region.

Paleoclimate setting

Variations in magnitude and latitudinal distribution of insolation are invoked as the major forcing mechanism for millennial-scale climatic variability during the Holocene in Eurasia (Harrison et al. 1996). In the Northern Hemisphere, between 12,000 and 6,000 year BP, variation in the latitudinal distribution of insolation anomalies reduced the latitudinal temperature gradient (Yu and Harrison 1995). Based upon atmospheric circulation patterns of the modern climate system, it is hypothesized that this reduced gradient shifted the latitude of westerly air mass penetration northward. An additional consequence of the insolation anomalies is the enhancement of land-sea temperature contrasts. This is likely to have increased the strength of both the winter Icelandic low and the summer Azores high, resulting in increased penetration of maritime air masses into the continental interior of Eurasia during both winter and summer (Harrison et al. 1992). Milder conditions in the interior also may have resulted from a decrease in anticylonic activity in the Arctic, which sustains the Siberian High during winter today.

Pollen records of late-glacial and Holocene climate generally follow the patterns predicted by variation in insolation. The late-glacial climate of the interior of northern Eurasia (Figure 1a) is inferred to have been cold and dry (Khotinskiy 1984), with tundra–steppe vegetation in the present-day forest zone of west Siberia (Blyakharchuk and Sulerzhitsky 1999). By 14,000 ^{14}C year BP (15,000 cal year BP), periglacial landscapes of the Ulagan Plateau in the central Altai were replaced by pioneer meadow-shrub-grass vegetation followed by a treeless dry steppe (Blyakharchuk et al. 2004).

Early-Holocene warmth is evidenced by widespread melting of permafrost and the northward expansion of the arctic treeline across northern Eurasia (Figure 1b). Macrofossil-and pollen-based reconstructions indicate the advance of *Betula*, *Larix*, *Picea*, and *Pinus* beyond their modern limits between 9,000 and 8,000 ^{14}C year BP (10,200 and 8,900 cal year BP) (Peteet et al. 1998; MacDonald et al. 2000; Davydova et al. 2001; Pisaric et al. 2001; Andreev et al. 2002; Väliranta et al. 2003). Early-Holocene warming is also indicated by an upslope movement of alpine treeline in the northern Urals (Kultti et al. 2003), by paleolimnological records from the northwest Siberian Arctic (Laing et al. 1999; Porinchu and Cwynar 2002), and by widespread initiation of peatland development in the West Siberian Lowland between 9,500 and 7,000 ^{14}C year BP (11,000 and 8,000 cal year BP) (Kremenetski et al. 2003). In the southeastern Altai, Ponomareva et al. (1991) and Butvilovsky (1993) suggest, based on macrofossil evidence, that altitudinal vegetation belts were 400–500 m higher. In the central Altai, the develop-

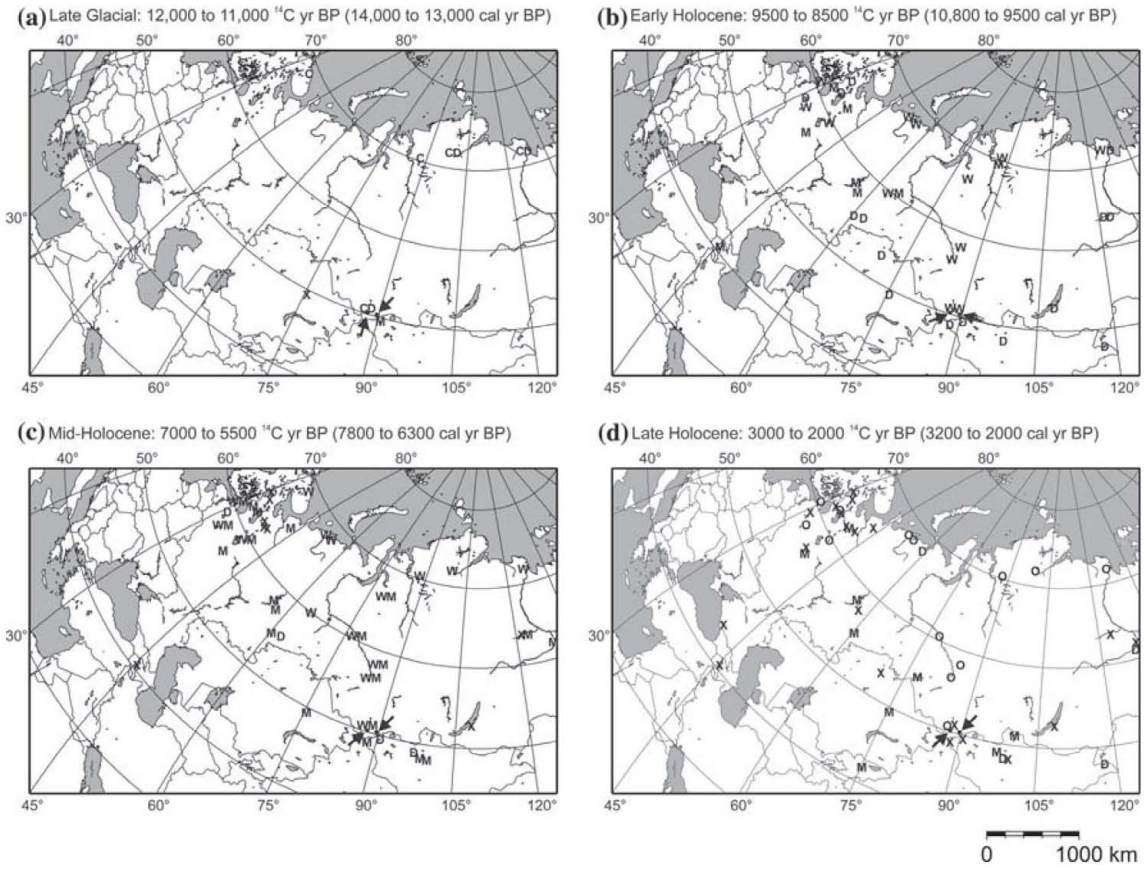

Figure 1. Summary diagram of published paleoclimate data (Ponomareva et al. 1991; Butvilovsky 1993; Harrison et al. 1996; Peteet et al. 1998; Blykharchuk and Sulerzhitsky 1999; Laing et al. 1999; MacDonald et al. 2000; Tarasov et al. 2000; Wolfe et al. 2000; Davydova et al. 2001; Pisaric et al. 2001; Andreev et al. 2002; Glebov et al. 2002; Blyakharchuk 2003; Fowell et al. 2003; Väliranta et al. 2003; Kultti et al. 2003; Blyakharchuk et al. 2004). Inferred climates for the (a) Late-glacial, (b) early-Holocene, (c) mid-Holocene, and (d) late-Holocene, as interpreted by the authors, are presented relative to modern climate. Letters denote direction of climate change: C = cooler, W = warmer, O = no temperature difference, M = higher effective moisture, D = lower effective moisture, and X = no moisture difference. Locations of this study's paleolimnological sites are denoted by arrows.

ment of closed forests featuring mesophilous species of *Picea* and *Abies* at elevations below 2,000 m (Blyakharchuk et al. 2004) imply a warmer and more humid climate. In contrast, paleolimnological records from sites in European Russia, Mongolia, and northeast Siberia indicate an early-Holocene climate that was drier than present, driven by greater-than-present summer insolation (Harrison et al. 1996; Wolfe et al. 2000; Davydova et al. 2001). The development of birch forest–steppe in southwest Siberia also indicates a warm and dry climate (Blyakharchuk 2003).

Climate reconstructions based on lake level (Harrison et al. 1996) and pollen (Tarasov et al. 1999) indicate enhanced moisture in most of northern Eurasia during the mid-Holocene (Figure 1c). The period from 7,000 to 5,000 ^{14}C year BP (7,800–5,700 cal year BP) is inferred to have been the warmest and most humid of the Holocene in Arctic Russia (Peteet et al. 1998; Wolfe et al. 2000; Davydova et al. 2001; Andreev et al. 2002) and western Siberia (Blyakharchuk and Sulerzhitsky 1999; Glebov et al. 2002; Blyakharchuk 2003). In west and southwest Siberia, dense forests replaced steppe communities during this period (Blyakharchuk and Sulerzhitsky 1999; Blyakharchuk 2003). In northwestern Mongolia, early-Holocene steppe was replaced by boreal coni-

fer steppe–forest by the mid-Holocene (Tarasov et al. 2000). Lakes in western Siberia, northwestern Mongolia, and northeastern Siberia suggest a more humid climate between 7,500 and 6,000 ^{14}C year BP (8,300 and 6,800 cal year BP) (Harrison et al. 1996; Tarasov et al. 2000). The only region where mid-Holocene climate is inferred to be relatively arid is in northern and central Mongolia, including Lake Telmen (Tarasov et al. 1999; Peck et al. 2002; Fowell et al. 2003).

Late-Holocene cooling led to the retreat of the arctic treeline to its modern position between 4,000 and 3,,000 ^{14}C year BP (4500 and ,3200 cal year BP) (MacDonald et al. 2000; Pisaric et al. 2001; Andreev et al. 2002; Väliranta et al. 2003) and, in western Siberia, to permafrost development and, in the south, renewed peat accumulation (Blyakharchuk and Sulerzhitsky 1999; Kremenetski et al. 2003) (Figure 1d). In the central Altai, a shift to a cooler and more continental climate is inferred from the near disappearance by 5,300 ^{14}C year BP (6,000 cal year BP) of *Abies* and *Picea* from the Ulagan Plateau (Blyakharchuk et al. 2004). In Mongolia, most lake-level records indicate decreased effective moisture after 6,000 ^{14}C year BP (6,800 cal year BP) (Harrison et al. 1996). However, at Lake Telmen, the period between 4,000 and 1,600 ^{14}C year BP (4,500 and 1,600 cal year BP) was the most humid of the Holocene, probably as a result of cooling (Peck et al. 2002; Fowell et al. 2003). A late-Holocene highstand is also recorded at Lake Hövsgöl in northern Mongolia (Fowell et al. 2003).

Study area

The rugged topography and continental setting of the Altai Mountains give rise to significant spatial variability in climate and a diversity of biomes. The most complete sequence of vegetation zones in Western Siberia is found in the Altai (Koropachinsky 1996). Enhanced moisture associated with orographic lifting promotes expansion of forest, which includes humid species *Abies sibirica* and *Picea obovata*, in the western and northern ranges. As mean annual precipitation decreases to the south and east, *Pinus sibirica* and *Larix sibirica* come to dominate. In these drier regions, the forest belt may disappear altogether, particularly on south-facing slopes (Malyshev and Nimis 1997). At higher elevations, a decline in alpine meadow vegetation and development of high-mountain tundra–steppe is associated with decreasing precipitation from west to east. Intermontane basins of the Russian Altai are characterized by steppe vegetation.

The three study lakes (Figure 2) are situated in landscapes that differ in precipitation, elevation, and vegetation. Dzhangyskol (50.18° N, 87.73° E; 1,830 m a.s.l.), a 60-ha lake located in Kurai basin, is situated adjacent to a pingo field and frozen fen. The modern lake is a remnant of a once larger ice-dammed lake that was partially drained during the early-Holocene (Blyakharchuk and Wright, unpublished data). The Kurkurek River, which does not flow into Dzhangyskol at present, flows along the southern boundary of the pingo field. Locally bordering Dzhangyskol is meadow-steppe vegetation, with *P. sibirica* and *L. sibirica* on surrounding slopes. Approximately 135 km to the east, Grusha Ozero (50.38° N, 89.45° E; 2,413 m a.s.l.) and Akkol (50.25° N, 89.62° E; 2,204 m a.s.l.) are situated in the high-elevation (2,000–2,500 m) Karaginskaya basin of southwestern Tuva, part of the Mongolian Interior Lakes drainage basin. Grusha Ozero is a 130-ha headwater lake situated within a belt of alpine tundra. Akkol, 350 ha and second in the lake chain, is surrounded by steppe vegetation. Table 1 provides a summary of climatic data from the three meteorological stations nearest to the study area. All three lakes are shallow (<4 m). Grusha Ozero and Akkol are circumneutral, oligomesotrophic lakes (Table 2). Limnological data are not available for Dzhangyskol.

Methods

Field

Sediment was recovered from the middle of the lakes with a square-rod piston corer (Wright Jr. 1991) in the summers of 1998 (Dzhangyskol) and 2000 (Grusha Ozero and Akkol). Unconsolidated surface sediments were obtained with a clear plastic tube fitted with a piston and sampled vertically in the field. At Dzhangyskol, 376 cm of sediment (64 cm gray silt overlain by 312 cm of alternating light calcareous and dark gyttja) were collected from the middle of the lake at a water depth of 1.2 m. A 48-cm segment of sediment from 212 to 260 cm was not recov-

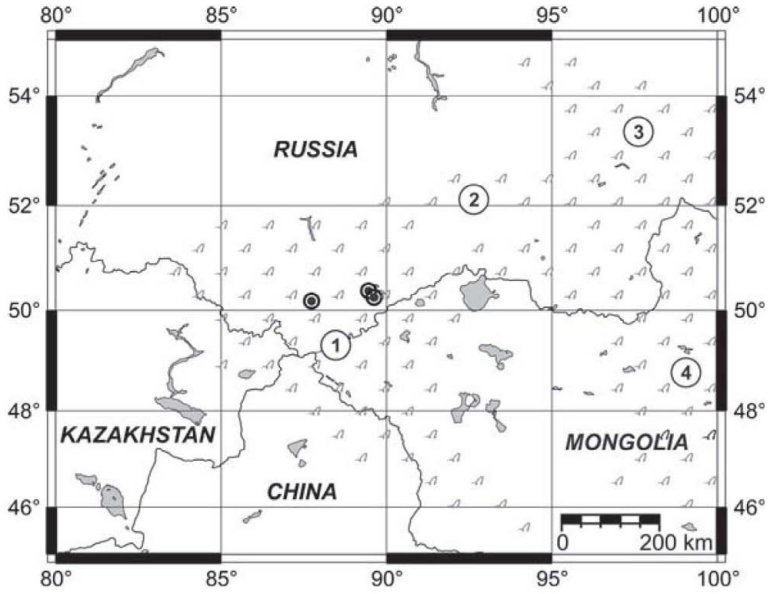

Figure 2. Map of study region, showing location of investigated lakes. Mountain ranges depicted are (1) Altai, (2) Western Sayan, (3) Eastern Sayan, and (4) Khangai.

Table 1. Climate data from Altai meteorological stations.

Meteorological station	Elev. (m)	Mean annual prec. (mm)	Mean January temp (C)	Mean July temp (C)	Days with mean T >10 C
Chemal (51.43° N, 86.00° E)	420	529	–12.4	18.1	131
Ust' Ulagan (50.70° N, 87.98° E)	1260	291	na	13.8	86
Kosh-Agach (50.02° N, 88.68° E)	1758	117	na	13.8	85

Data compiled from Malyshev and Nimis (1997), WWF Climate Program (2001), and Groisman (1998).

ered. At Grusha Ozero, 249 cm of sediment were obtained from a water depth of 3.55 m. The sediment was composed of 13 cm of gray silt overlain by 236 cm of light and dark brown gyttja. At Akkol, 470 cm of sediment were recovered from a water depth of 2.8 m. The sediment consisted of 68 cm of silty clay overlain by 402 cm of olive-gray gyttja.

Table 2. Measured nutrients, total organic carbon (TOC), and pH from Grusha Ozero and Akkol.

	Grusha Ozero	Akkol
TN (mg/l)	9.1	9.1
TP (µg/l)	13.7	12.7
H_4SiO_4(mg/l)	2.9	3.3
TOC (mg/l)	0.3	0.4
pH	6.5	7.3

Water chemistry data is not available for Dzhangyskol.

Laboratory

Sediments were sampled at semi-regular intervals for loss-on-ignition, pollen, chironomids, biogenic silica and diatom analyses. Surface cores were sampled in 1-cm increments at 5 cm intervals, with the exception of the Dzhangyskol surface core, which was sampled in contiguous 1-cm sections for the first 20 cm and contiguous 2-cm sections for the bottom 40 cm. The sub-surface piston cores were sampled in 1-cm increments at varying intervals based on apparent differences in sedimentation rate both between and within cores. The sampling resolution of diatoms and biogenic silica, reported in this manuscript, was dictated by sample availability.

Terrestrial macrofossils, charcoal, and bulk sediment also were collected for ^{14}C dating by accelera-

tor mass spectrometry (AMS). Calibrated ages were determined by CALIB 4.4 (Stuiver and Reimer 1993; Stuiver et al. 1998a, b) based on a 2σ error. Results are reported in Table 3.

Lake sediments were analyzed following standard procedures for loss-on-ignition at 550 and 950 °C as an estimation of organic matter and carbonate content, respectively (Heiri et al. 2001).

Biogenic silica

Biogenic silica (BSi) determinations were made via wet-alkaline extraction (DeMaster 1979). Approximately 30 mg of freeze-dried sediment, homogenized by mortar and pestle, were digested with a weak base (1% Na_2CO_3)at 85 °C in a water-bath shaker. Aliquots were withdrawn every hour for 5 h. Dissolved silica concentrations of the aliquots were determined spectrophotometrically with a Cary Bio 100 UV–visible Spectrophotometer, based on the formation of a blue silicomolybdate complex. Because some leaching of mineral silicates commonly occurs, the intercept of a least-squares linear regression of dissolved silica concentration at 3, 4, and 5 h was used to estimate BSi concentration (Conley 1998; Conley and Schelske 2001). Where there was no increase in dissolved silica concentration with time, the mean of the 3, 4, and 5 h extractions was used to estimate biogenic silica concentration. As a check on both internal consistency and consistency with other laboratories, an interlaboratory comparison sample was included with each batch of samples. Measured BSi concentrations for this sample were within one standard deviation of that reported by Conley (1998).

BSi is a proxy for diatom abundance and may reflect diatom productivity (Conley and Shelske 2001). BSi concentrations, however, may not accurately reflect paleoproductivity if sedimentation rates are variable over the period of record. Therefore, mass accumulation rates of BSi were calculated for Akkol, which has a well constrained chronology, based on sediment dry density, estimates of linear sedimentation rate, and BSi concentration.

Diatoms

Following treatment in 10% hydrochloric acid and 35% hydrogen peroxide to remove carbonates and organic matter, respectively, diatom samples were mounted on glass slides with Naphrax® and examined at 1000× under oil immersion with a Zeiss Axioskop 2 light microscope. Diatom assemblages were characterized by counts of 300–500 valves, with a single exception where only 105 intact valves were encountered in 10 transects across the slide. Scanning Electron Microscopy (JEOL JSM-T330) was also used to resolve uncertainties in species identifications. Taxonomic identifications were made with reference to multiple taxonomic references, including Krammer and Lange-Bertalot (1986–1991), Camburn and Charles (2000), Lange-Bertalot and Metzeltin (1996), Fallu et al. (2000), Williams and Round (1987), and Haworth (1974).

Two standard alpha diversity indices, Shannon diversity (H') and Evenness (E) were employed to explore how diatom community structure has changed throughout the lakes' histories.

$$H' = -\sum_{i=1}^{S} p_i \ln p_i \quad (1)$$

$$E = \frac{H'}{\ln S} \quad (2)$$

S = total number of species, p_i = proportion of the ith species.

Specimens that could not be identified to at least the species level (usually for reasons of preservation) were excluded in the determination of sample diversity. Varieties were considered as separate and distinct taxa in diversity analysis.

Multivariate numerical analyses

The rarest taxa, as well as those that could not be identified to species level, were excluded from numerical analysis. Only species or varieties occurring in relative abundances of at least 2% in one sample were retained. A total of 49 taxa were retained in the Dzhangyskol dataset, 26 in the Grusha Ozero dataset, and 14 in the Akkol dataset. These retained taxa accounted for 76–99% (median 91%) of the Dzhangyskol assemblages, 74–99% (median 92%) of the Grusha Ozero assemblages, and 72–100% (median 96%) of the Akkol assemblages.

Table 3. Radiocarbon analysis results.

Sample number	Lake	Sediment depth (cm)	Lithology	Material	Age ^{14}C year BP	Age (cal year BP)	Age range (cal year BP)
CURL5329	Dzhangyskol	93–96	Gyttja	Larix, needle	4150 ± 40	4690	4570–4830
CURL5328	Dzhangyskol	136–140	Gyttja	Rumex, Larix, chenopod seeds	4830 ± 40	5550	5470–5650
AA45774	Dzhangyskol	145–147	Gyttja	Charcoal	7020 ± 200	7850	7550–8200
Poz4404	Dzhangyskol	154–155	Marl	Charcoal	8170 ± 50	9130	9010–9280
AA45773	Dzhangyskol	163–165	Gyttja	Sedge	11360 ± 710	13390	11540–15440
CURL5974	Dzhangyskol	169–176	Gyttja	Larix needles, Betula fruit, charcoal	8660 ± 140	9710	9470–10150
CURL4012	Dzhangyskol	187–188	Gyttja	Carex seed, bark	10750 ± 60	12830	12620–13000
CURL4349	Dzhangyskol	209–210	Gyttja	Betula fruit, charcoal	10820 ± 190	12850	12300–13190
CURL4013	Dzhangyskol	290–292	Gyttja	Larix needle, charcoal	9890 ± 60	11280	11170–11360
CURL4014	Dzhangyskol	305–308	Gyttja	Chenopod seed, wood, charcoal	10150 ± 60	11780	11550–12150
CURL4015	Dzhangyskol	344–346	Silt	Charcoal	10450 ± 90	12450	12050–12830
CURL5550	Grusha Ozero	55	Gyttja	Bulk sediment	6060 ± 40	6900	6790–7010
CURL5551	Grusha Ozero	95	Gyttja	Bulk sediment	8120 ± 45	9070	8990–9260
AA44429	Grusha Ozero	130	Gyttja	Bulk sediment	9655 ± 87	10950	10740–11200
CURL5552	Grusha Ozero	135	Gyttja	Bulk sediment	9710 ± 50	11130	10860–11230
AA44430	Grusha Ozero	145	Gyttja	Bulk sediment	9834 ± 74	11230	11110–11360
AA44431	Grusha Ozero	155	Gyttja	Bulk sediment	10008 ± 70	11480	11230–11700
AA44433	Grusha Ozero	155	Gyttja	Macrofossil	10003 ± 78	11480	11220–11760
AA44432	Grusha Ozero	165	Gyttja	Bulk sediment	9691 ± 76	11050	10750–11230
AA44434	Grusha Ozero	165	Gyttja	Macrofossil	9617 ± 76	10930	10730–11170
CURL5553	Grusha Ozero	175	Gyttja	Bulk sediment	9770 ± 65	11180	11070–11260
AA44435	Grusha Ozero	185	Gyttja	Plantfibers	9860 ± 100	11280	11090–11650
CURL5554	Grusha Ozero	195	Gyttja	Bulk sediment	10270 ± 55	12070	11690–12380
CURL5555	Grusha Ozero	210	Gyttja	Bulk sediment	10710 ± 50	12800	12620–12970
CURL5556	Grusha Ozero	225	Gyttja	Bulk sediment	11330 ± 55	13290	13140–13480
CURL5557	Grusha Ozero	232	Gyttja	Bulk sediment	11820 ± 60	13860	13470–14090
CURL5558	Grusha Ozero	239	Silt	Bulk sediment	12370 ± 55	14660	14120–15420
CURL5536	Akkol	36	Gyttja	Bulk sediment	2150 ± 45	2140	2000–2310
CURL5537	Akkol	95	Gyttja	Bulk sediment	3580 ± 50	3870	3720–3990
CURL5538	Akkol	154	Gyttja	Bulk sediment	4660 ± 35	5400	5310–5470
CURL5539	Akkol	214	Gyttja	Bulk sediment	5320 ± 40	6080	5990–6200
CURL5540	Akkol	276	Gyttja	Bulk sediment	6210 ± 60	7100	6950–7250
CURL5546	Akkol	325	Gyttja	Bulk sediment	6950 ± 50	7760	7670–7860
CURL5547	Akkol	386	Gyttja	Bulk sediment	8100 ± 45	9050	8980–9130
AA44428	Akkol	414	Silt	Bulk sediment	8491 ± 68	9490	9400–9560
CURL5548	Akkol	424	Silt	Bulk sediment	8460 ± 50	9480	9420–9540
AA44427	Akkol	428	Silt	Bulk sediment	12320 ± 130	14600	14080–15400
AA44426	Akkol	432	Silt	Bulk sediment	9980 ± 100	11470	11180–11770
CURL5549	Akkol	438	Silt	Bulk sediment	11450 ± 55	13380	13160–13510

^{14}C ages were calibrated using CALIB 4.4 (Stuiver and Reimer 1993; Stuiver et al. 1998a, b) based on 2σ error. Radiocarbon analyses were performed at three laboratories, identified by the letters beginning the sample identification codes. AA = NSF Arizona AMS Laboratory, USA; CURL = INSTAAR AMS Laboratory, Colorado, USA; Poz= Poznan Radiocarbon Laboratory, Poland.

Diatom assemblage zones were defined by stratigraphically constrained cluster analysis by the incremental sum of squares (CONISS) algorithm using psimpoll 4.10 (Bennett 2002). Prior to analysis, species relative abundance data were square-root transformed, and the resultant dissimilarity coefficient is chord distance. The effect of the transformation is to maximize the signal-to-noise ratio in the data by upweighting subdominant taxa and is considered most appropriate for species abundance data (Overpeck et al. 1985). The number of statistically significant zones was determined by the broken-stick model (Bennett 1996).

Ordination analysis was employed to identify theoretical gradients that best explain observed variability in the diatom species data. Detrended Correspondence Analysis (DCA) with down-weighting of rare taxa, detrending by segments, and linear rescaling was performed on relative abundance data using CANOCO 4.5 (ter Braak and Šmilauer 1998). DCA revealed gradient lengths of 2.55, 1.94, and 1.06 standard deviation (SD) units for Dzhangyskol, Grusha Ozero, and Akkol, respectively. Because none of these gradients exceeded 3 SD units, Principal Components Analysis (PCA) was selected as the most appropriate ordination method (Lepš and Šmilauer 2003). PCA was performed on the covariance matrix of the diatom relative abundance data with no other transformation.

Results

Dzhangyskol

Chronology

The eleven radiocarbon dates obtained from the Dzhangyskol core (Table 3) reflect the lake's complex depositional history, a full discussion of which is in preparation by Blyakharchuk and Wright. The three oldest dates (163–210 cm) are interpreted to be reworked late-glacial material deposited during a low stand, following failure of the ice dam that created the lake. An unconformity is inferred from the lack of material between approximately 5,500 and 7,500 cal year BP in age. Age of sediments is estimated by linear interpolation for intervals preceding and following the depositional hiatus (Figure 3a).

Loss-on-ignition

As estimated by loss-on-ignition at 550 °C (LOI_{550}), organic-matter content is very low from the base of the core to 308 cm (~11,800 cal year BP) (Figure 4a), corresponding to the basal silt. Subsequently organic-matter content increases to nearly 50% at 270 cm (~11,000 cal year BP). There is an abrupt decrease in organic-matter content and an increase in carbonate content, inferred from loss-on-ignition at 950 °C (LOI_{950}), at 269 cm. This change in sediment character is reflected in a transition from a dark gyttja to a gray calcareous gyttja. Between 269 and 96 cm (~11,000–4,700 cal year BP), organic-matter content is variable, ranging from 8 to 41%. Fluctuations in the percent LOI_{950} between 4 and 32% also occur in this interval, indicating the presence of carbonates in significant amounts. Above and below this interval, the percent LOI_{950} never exceeds 4%, and carbonate content is insignificant. Above 96 cm, organic-matter content declines until 64 cm (~3,200 cal year BP). From 64 cm, organic-matter content steadily increases to 63% at 5 cm (~200 cal year BP).

Biogenic silica

For much of the sedimentary record, BSi concentrations are low (Figure 4a). Below 96 cm (~4,700 cal year BP), BSi never exceeds 50 mg g^{-1}. BSi increases to 100 mg g^{-1} by 80 cm (~4,000 cal year BP). Between 48 and 59 cm (~2,400 and 2,900 cal year BP), BSi concentrations decline before increasing once more to levels near 100 mg g^{-1}. Maximum BSi concentrations of ~140 mg g^{-1} occur in two samples from 17 to 19 cm (~800–900 cal year BP).

Diatoms (Figure 5)

DZH-1 (48–308 cm, 2,400–11,800 cal year BP). A gap in sediment recovery of 48 cm, which represents ~700 years of the early-Holocene, divides this zone into two subzones, 261–308 cm and 48–210 cm. Diatoms first appear in abundance at 308 cm. Below this depth, diatom valves are extremely rare and usually broken. This zone is characterized by large inter-sample variability. At 308 cm, the assemblage is dominated by the benthic colonial species *Pseudostaurosira binodis* (Ehrenberg) Edlund, which is found occasionally in much lower abundances in the rest of the core. The diatom assemblage is subsequently characterized by a short-lived but marked

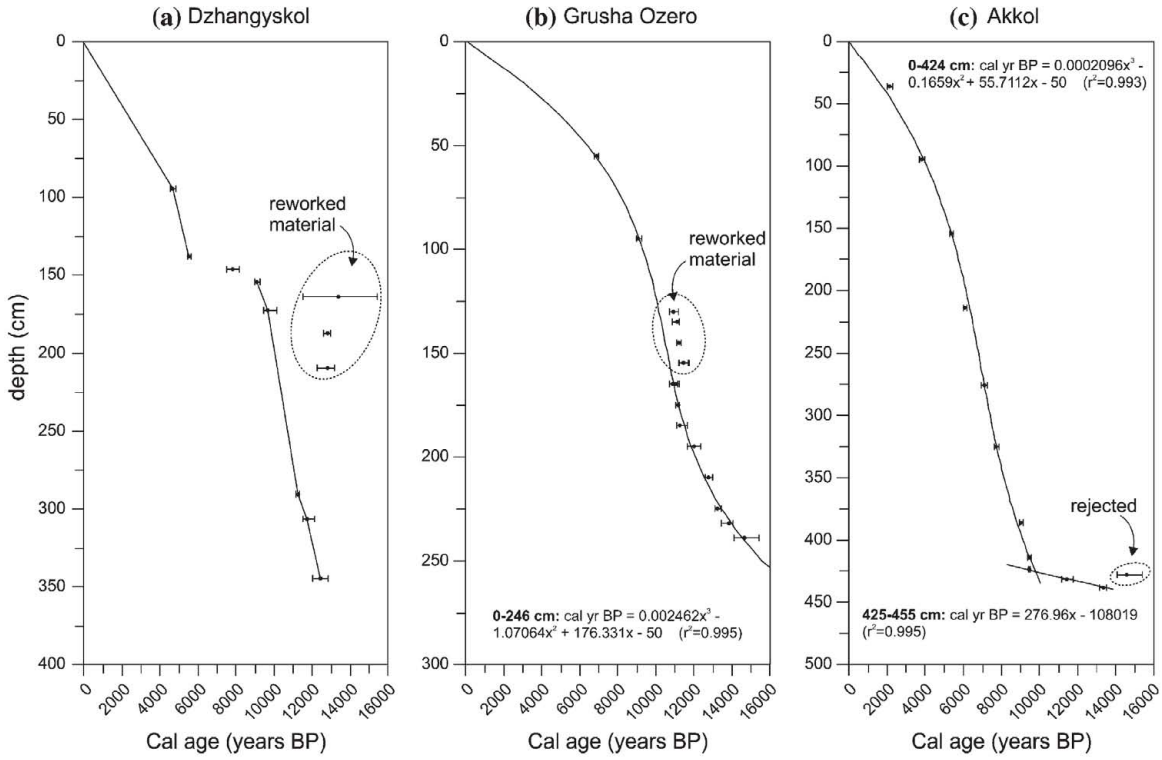

Figure 3. Age-depth models of the study lakes. The age of Dzhangyskol sediment, above and below an inferred hiatus at approximately 140 cm, is estimated by linear interpolation between calibrated radiocarbon samples. Three stratigraphically inverted dates in Dzhangyskol are interpreted as late-glacial material redeposited following the failure of an ice dam and partial draining of the lake. Fitted polynomial age models are given for Grusha Ozero and Akkol. Five Grusha Ozero dates, between 130 and 155 cm, interpreted as redeposited sediment, are excluded from that model.

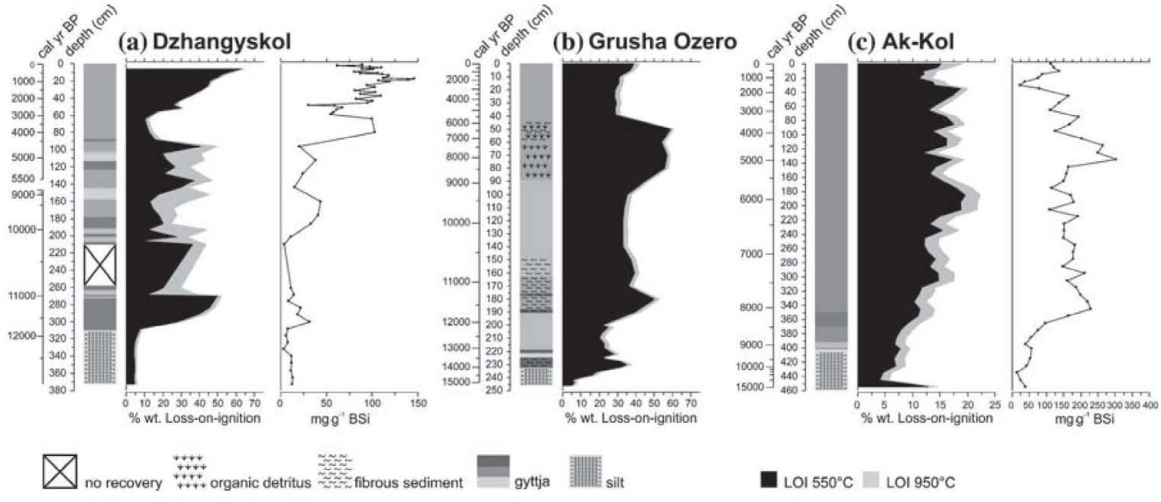

Figure 4. Lithology and stratigraphic profiles of loss-on-ignition and biogenic silica for (a) Dzhangyskol, (b) Grusha Ozero (no BSi), and (c) Akkol, plotted as a function of depth. Non-linear age scales are also provided to the left of each profile.

increase in diversity at 300 cm (~11,600 cal year BP). The most abundant taxa, which range in relative abundance from 11 to 7%, respectively, are *Achnanthidium minutissimum* (Kützing) Czarnecki (all varieties), *Cocconeis placentula* v. *lineata* (Ehrenberg) Van Heurck, *Cymbella leptoceros* (Ehrenberg)

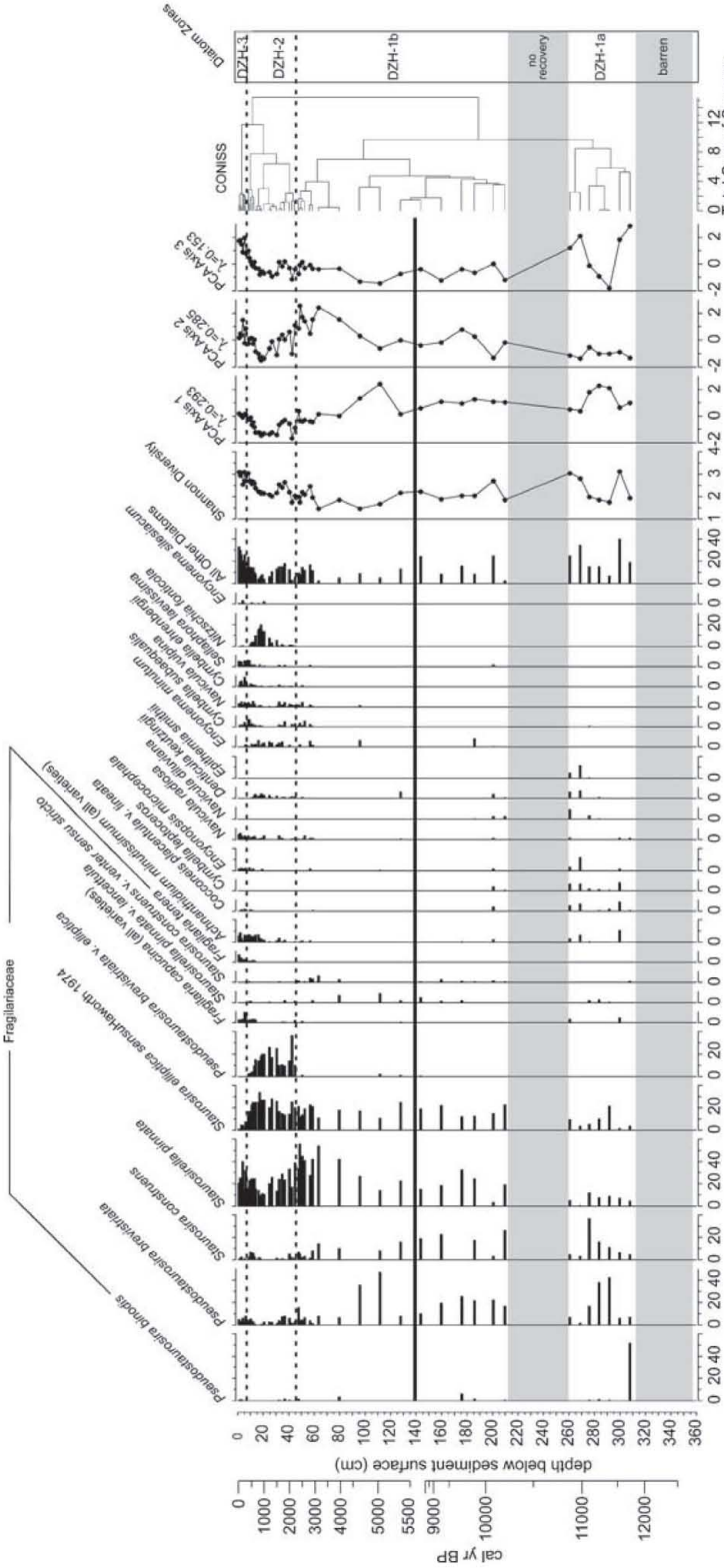

Figure 5. Dzhangyskol Diatom Stratigraphy. Species with relative abundances greater than 5% are plotted. The Shannon diversity index and sample scores for the first three PCA axes are also plotted. Evenness is not displayed as it is highly correlated ($r = 0.93$, $p \ll 0.001$) with the Shannon index. Zonation is based on the CONISS algorithm with significant clusters identified by the broken-stick model. An inferred hiatus at 140 cm denoted by a thick line.

Kützing, and *Staurosirella pinnata* (Ehrenberg) Williams & Round. Thereafter, assemblages are characterized by increased abundances of benthic colonial Fragilariaceae taxa including *Pseudostaurosira brevistriata* (Grunow in Van Heurck) Williams & Round, *Staurosira construens* Ehrenberg, and *Staurosira elliptica* (Schumann) Williams & Round sensu Haworth 1974. At 269 cm (~11,000 cal year BP), the dominant Fragilariaceae taxa decline and diversity increases once again, with *Navicula diluviana* Krasske, *Epithemia smithii* Carruthers, *Encyonopsis microcephala* (Grunow) Krammer, and *Denticula keutzingii* Grunow occurring at their maximum abundances. Taxa important during the earlier rise in diversity also increase in abundance once again. Subzone DZH-1b is defined by the return to dominance of Fragilariaceae taxa, including *P. brevistriata*, *S. pinnata*, *S. elliptica*, and *S. construens*. *Staurosirella pinnata* increases in abundance at the top of this zone, while abundances of *P. brevistriata* and *S. construens* decline. The dominance of these Fragilariaceae taxa produces the lowest average value in the diversity indices of the entire record. At 60 cm (~3,000 cal year BP), diversity increases, with occurrences of *Cymbella subaequlis* Grunow, *Encyonema minutum* (Hilse ex Rabenhorst) Mann, *Navicula radiosa* Kützing, and *Navicula vulpina* Kützing.

DZH-2 (8–46 cm, ca. 350–2300 cal year BP). This zone is characterized by the first significant occurrence of *P. brevistriata* v. *elliptica* (Héribaud) Williams & Round, with *S. elliptica* as co-dominant. *Staurosirella pinnata* declines during this period. The top of this zone (8–14 cm, ca. 350–650 cal year BP) is transitional to zone DZH-3, featuring decreasing abundance of *P. brevistriata* v. *elliptica* and *S. elliptica*, increasing abundance of *S. pinnata*, and a trend of increasing diversity. This zone is also characterized by the rise and subsequent decline in abundance of *Nitzschia fonticola* Grunow. Additional taxa emerging in increased relative abundance in this zone include *Fragilaria capucina* Desmazières (all varieties), *A. minutissimum* (all varieties), *D. keutzingii*, and *Sellaphora laevissima* (Kützing) Mann.

DZH-3 (1–7 cm, 0–ca. 300 calendar years BP). This zone is characterized by diversity second only to that of the earliest assemblages. Of the small benthic colonial taxa, only *S. pinnata* is present in significant abundance. *Fragilaria tenera* (W. Smith) Lange-Bertalot and *Cymbella ehrenbergii* Kützing reach their maximum abundances in this zone.

Principal components analysis. The first three PCA axes explain 73% of the variability in the species assemblage data (Table 4). The gradient represented by PCA axis 1 primarily reflects variations in the abundance of *P. brevistriata*, *S. construens*, and *P. brevistriata* v. *elliptica*. Some of the variation in *S. elliptica* is also captured in this axis. Also reflected in this axis is long-term change in the composition of sub-dominant taxa, which occur in abundances of 2–20% and can be visualized on the stratigraphic diagram as a shift to the right as one moves up the stratigraphic column. The second ordination axis, which explains nearly the same amount of variability as the first, most strongly reflects variation in *S. pinnata* ($r = 0.97$), a dominant species for most of the Dzhangyskol record. The third ordination axis primarily reflects species diversity, with positive loadings on subdominant taxa and negative loadings of dominant taxa, particularly *S. elliptica*, and is positively correlated with both diversity indices ($r = 0.63$ and 0.74, $p < 0.001$).

Table 4. Summary of principal components analysis (PCA) results.

	No. species	Eigenvalues (cumulative percentage of variance explained)		
		Axis 1	Axis 2	Axis 3
Dzhangyskol	49	0.293 (29.3)	0.285 (57.8)	0.153 (73.1)
Grusha Ozero	26	0.761 (76.1)	0.135 (89.7)	0.030 (92.7)
Akkol	14	0.540 (54.0)	0.239 (77.8)	0.139 (91.7)

Species or varieties occurring in relative abundances of at least 2% in one sample were included in the PCA, which was performed on the covariance matrix of relative abundance data.

Grusha Ozero

Chronology

The chronology of the Grusha Ozero core is based on 16 radiocarbon dates (Table 1). In two instances, dates on macrofossils and bulk sediment collected from the same depth show overlapping calibrated age ranges. Median ages ranging from 10,930 to 11,480 cal year BP are reported from nine samples taken at seven depths between 130 and 185 cm. Several of these dates are out of stratigraphic order but overlap in their ranges. The five dates between 130 and 155 cm appear too old, perhaps from the redeposition of shallow water sediments caused by climate-driven changes in lake-level. On that basis, we have excluded these dates from our age model. An age model ($r^2 = 0.99$) was created by fitting a third-order polynomial to the remaining median calibrated age estimates (Figure 3b).

The oldest material from Grusha Ozero dates to 14,660 cal year BP. The model suggests a period of relatively rapid sediment accumulation between ~12,000 and 10,000 cal year BP (200–120 cm). The greatest uncertainty in this model lies in dating of the youngest sediments. The youngest sample (55 cm) dates to 6,900 cal year BP, which implies either a very slow sediment accumulation rate at the top of the sequence or an undetected hiatus in sedimentation.

Loss-on-ignition

LOI_{550} is less than 10% below 240 cm (~14,600 cal year BP) but exceeds 20% above 234 cm (~14,100 cal year BP) (Figure 4b). LOI_{550} maxima between 232 and 228 cm (~14,000–13,700 cal year BP), 190 and 150 cm (~11,700–10,600 cal year BP), and 90–50 cm (~9,000–6,400 cal year BP) correspond to fibrous sediment, the presence of fine and coarse detritus, and darker color. Maximum organic-matter content of 59% occurs at 50 cm (6,400 cal year BP). Above 50 cm, organic-matter content is stable at ~30% until a recent (~last 800 cal year BP) increase. LOI_{950} is low throughout the core, never exceeding 3%, indicating little or no carbonate.

Diatoms (Figure 6)

GR-1 (200–236 cm, 12,100–14,300 cal year BP). Diatoms first occur at 236 cm. Diatoms are absent from 234 to 228 cm but reappear at 226 cm. This zone is composed predominantly of the small benthic Fragilariaceae taxa *S. elliptica* and *S. pinnata*. Initially, this zone is characterized by a higher proportion of *S. elliptica* and low diversity. The latter half of the zone is distinguished by increased abundance of *S. pinnata*, *S. construens*, *P. pseudoconstruens*, and *P. brevistriata* and the first significant appearance of non-Fragilariaceae taxa.

GR-2 (155–195 cm, 10,700–11,900 cal year BP). *Staurosirella elliptica* is the most abundant taxon in this zone, which features step reductions in the abundance of *S. pinnata* and increased abundance of *P. brevistriata*. Species diversity is highest in this zone. A brief occurrence of *S. pinnata* v. *intercedens* (Grunow) Williams & Round between 195 and 175 cm (~11,900 and 11,200 cal year BP) and new occurrences of non-Fragilariaceae taxa above 175 cm also characterize zone GR-2. Important sub-dominant taxa in this zone include *C. placentula* v. *lineata*, *Amphora pediculus* (Kützing) Grunow, *C. leptoceros*, *A. minutissimum* (all varieties), *Navicula vitabunda* Hustedt, *Navicula subrotundata* Hustedt, and *Cyclotella ocellata* Pantocsek.

GR-3 (50–150 cm, 6,400–10,600 cal year BP). On average, this zone is characterized by the lowest diversity index values of the entire record. However, this is due largely to the extreme dominance of *S. elliptica*, particularly above 95 cm (~9,200 cal year BP). *Staurosirella pinnata*, which had previously been co-dominant, is found in low abundance. *Pseudostaurosira brevistriata* continues to be important, although its abundance decreases above 95 cm. *Navicula diluviana* appears as an important taxon numerically, with peak abundances below 95 cm. *Cyclotella ocellata* also disappears above 95 cm.

GR-4 (0–45 cm, 0–6,000 cal year BP). This zone features an abrupt increase in the abundance of *S. pinnata*, largely replacing *S. elliptica* as the dominant species. It is also characterized by the reappearance of *P. pseudoconstruens* and the first significant appearance of *Synedra parasitica* (W. Smith) Hustedt. Two samples, representing the past 800 years, show co-dominance of *S. elliptica*, *S. pinnata*, and *S. construens*. Diversity remains relatively low, with rare

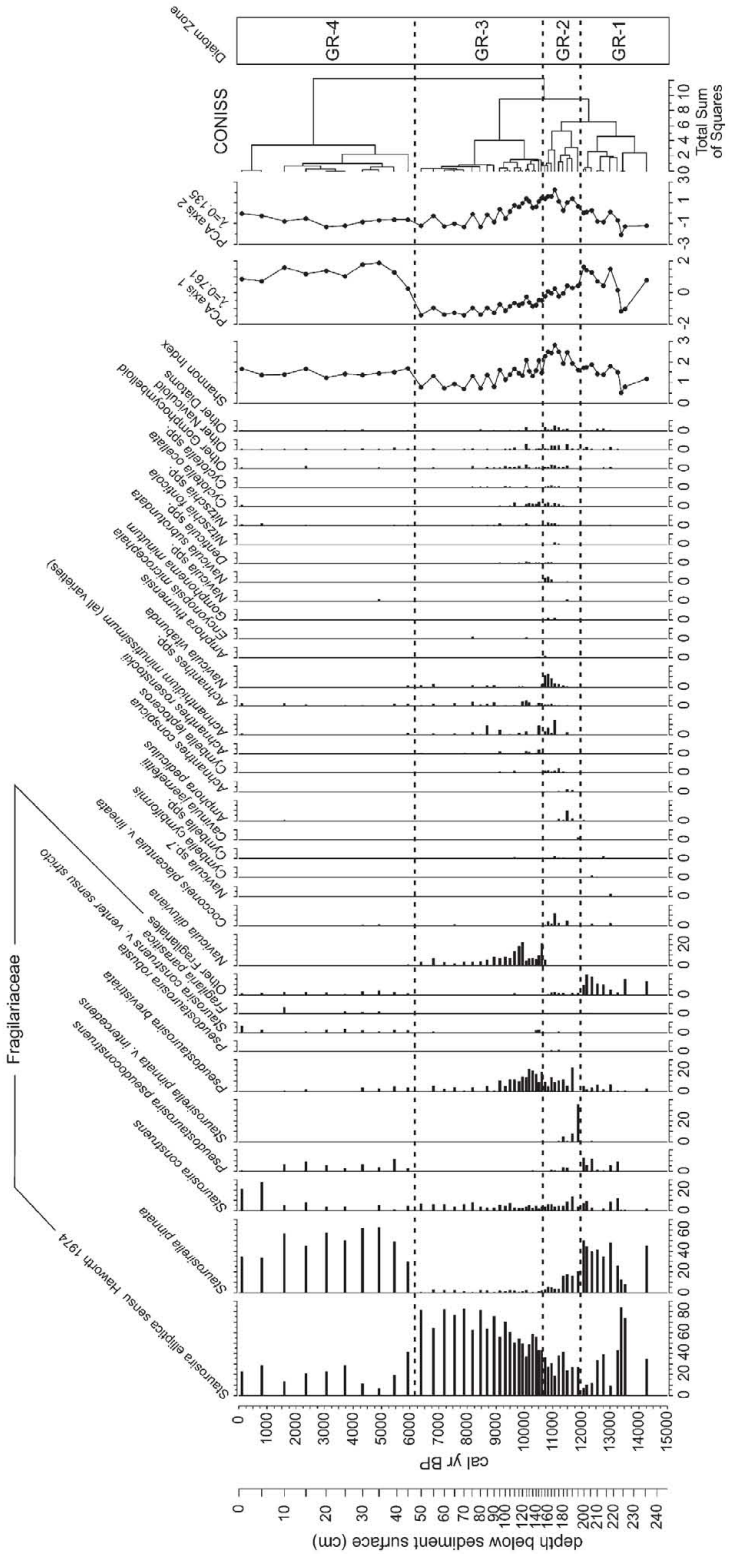

Figure 6. Grusha Ozero Diatom Stratigraphy. Species with relative abundances greater than 2% are plotted, as are the Shannon diversity index and the sample scores for the first two PCA axes. Evenness is not displayed as it is highly correlated ($r = 0.89$, $p \ll 0.001$) with the Shannon index. Zonation is based on the CONISS algorithm with significant clusters identified by the broken-stick model.

occurrences of *C. ocellata, Achnanthes*, *Nitzschia*, Naviculoid, and Gomphocymbelloid taxa.

Principal components analysis. The first two PCA axes explain 90% of the variability in the species assemblage data (Table 4). Most of this variation is captured in the first ordination axis, which reflects variation in the abundance of *S. pinnata* ($r = 0.92$, $p \ll 0.001$) and *S. elliptica* ($r = -0.94$, $p \ll 0.001$). Major shifts in axis 1 correspond to zone boundaries. PCA axis 2 primarily reflects variation in abundance of a number of sub-dominant taxa, including *P. brevistriata* and a number of non-Fragilariaceae taxa and is positively correlated to the Shannon index of species diversity ($r = 0.83$, $p \ll 0.001$).

Akkol

Chronology

The chronology of the Akkol core is based on 12 radiocarbon dates (Table 3). One date, at 428 cm, is out of stratigraphic order. This sample provides the oldest date and has the largest uncertainty. Given the good fit of three other dates between 424 and 438 cm, we have excluded this date from the age model. The chronology is composed of two separate age models to account for an abrupt change in sedimentation rate at approximately 425 cm (~9,700 cal year BP) (Figure 3c). The first model, which applies from 0 to 424 cm, is a third-order polynomial fit to nine dates with an r^2 of 0.99. The second model, which applies from 425 to 438 cm, is a linear fit of three dates with an r^2 of 0.99. Below 438 cm, the chronology is uncertain, constrained only by a minimum age of 13,400 cal year BP.

Loss-on-ignition

Organic matter ranges from 4 to 20% by weight (Figure 4c). Except for a single high value of 13% at the base of the core, organic matter shows an increasing trend to its peak at 185 cm (~5,900 cal year BP). Subsequently, organic-matter content varies between 11 and 19% with no significant trend. LOI_{950}, which may represent carbonates or dehydration of clay minerals, is low throughout the record, ranging from 1.3 to 3.7%. No carbonates are present in the bedrock or glacial materials in the area.

Biogenic silica

BSi concentrations are low (less than 60 mg g^{-1}) from the base of the core to 385 cm (~8,800 cal year BP), then increase rapidly to 230 mg g^{-1} by 345 cm (~8,000 cal year BP) (Figure 7). Above 345 cm, BSi concentrations range between 110 and 220 mg g^{-1}, before increasing abruptly again to a maximum concentration of 300 mg g^{-1} by 135 cm (~5,000 cal year BP). Above 135 cm, BSi concentrations show a decreasing trend that is punctuated by peaks at 75 and 45 cm (~3,300 and 2100 cal year BP). BSi concentrations reach a late-Holocene minimum of 20 mg g^{-1} at 30 cm (~1,500 cal year BP) but increase to 140 mg g^{-1} by 10 cm (~500 cal year BP) and have changed little since then.

BSi is positively correlated ($r = 0.503$, $p = 0.0002$) with organic-matter content, as estimated by LOI_{550}, suggesting that sedimentary BSi may be a proxy for diatom productivity in Akkol. The application of sedimentary BSi as a proxy for paleoproductivity also assumes that silica was not limiting over the period of record and therefore is most appropriately applied in oligotrophic systems (Conley and Schelske 2001), a reasonable assumption in this case.

BSi accumulation rates range from a minimum of 0.04 to 5.0 mg cm^{-2} $year^{-1}$. BSi accumulation is lowest in the silty sediment at the base of the core and in the top 35 cm (last 1,700 years). Maximum accumulation rates occur between 335 and 315 cm (~7,900–7,600 cal year BP) and subsequently show a gradual declining trend (Figure 7). Sub-millennial scale variations are also apparent against the background of declining BSi accumulation rates.

Diatoms (Figure 8)

The diatom record of Akkol is characterized by low diversity (i.e., few taxa in significant abundances) and minimal stratigraphic variation. By comparison, the complete Akkol record shows approximately the same magnitude of variability as a single zone within the Dzhangyskol and Grusha Ozero records.

AK-1 (145–455 cm, 5,200–15,000 cal year BP). This zone is co-dominated by *S. elliptica* and S. *pinnata*. Pseudostaurosira *brevistriata* and S. construens are sub-dominant. Diversity is low except for a single sample (435 cm) that corresponds to

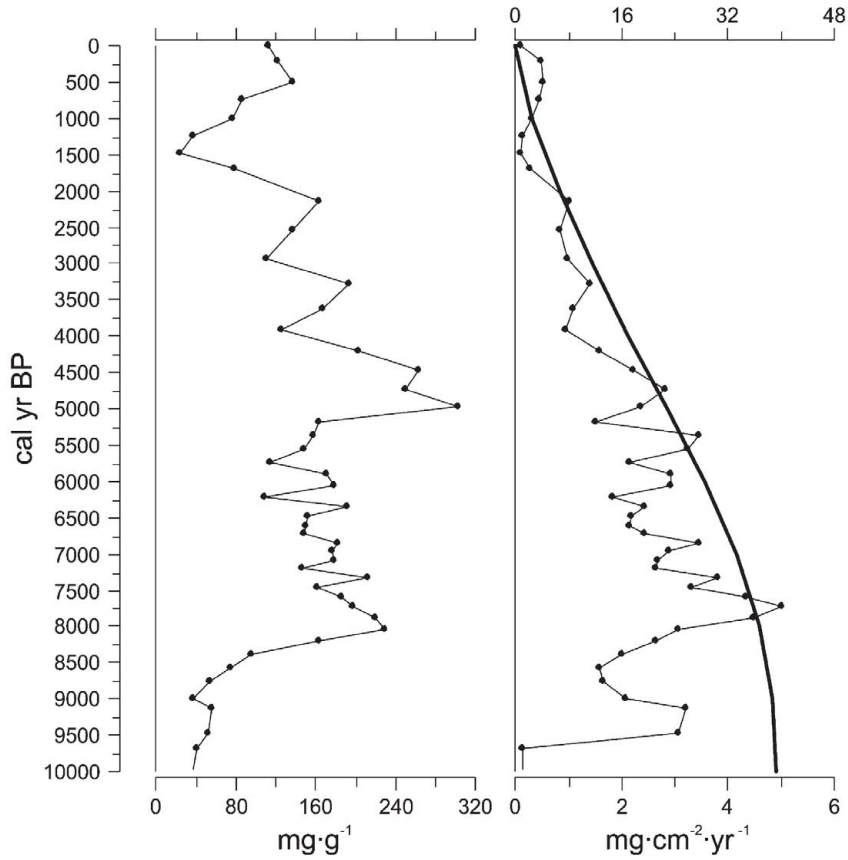

Figure 7. Akkol biogenic silica concentration and accumulation rates for the last 10,000 years. July insolation at 50 °N (Berger and Loutre 1991) is plotted as deviations relative to present.

the period of low sedimentation during the late-glacial/early-Holocene. Another sample from this period (445 cm) was barren of diatoms. For a brief interval between 295 and 275 cm (~7,000–7,300 cal year BP), *S. construens* reaches maximum abundances of 33–40%.

AK-2 (45–135 cm, 2,000–5,000 cal year BP). This zone is distinguished by increased abundance of *S. pinnata* and reduced abundance of *S. elliptica* and *P. brevistriata*.

AK-3 (0–35 cm, 0–1,700 cal year BP). Staurosirella pinnata persists as the dominant taxon in zone AK-3. This zone is distinguished by further decline in the abundance of *S. elliptica*, reduced abundance of *S. construens*, and increasing abundances of *P. brevistriata*. Species diversity is at a maximum, especially from 0 to 20 cm (~last 1,000 years) as non-Fragilariaceae taxa occur with greater frequency. This is also the only period of the record when the Shannon and Evenness indices are significantly correlated (r = 0.78, p = 0.02).

Principal components analysis. The first three axes explain 92% of the variation in the stratigraphic record (Table 4). More than half of the variation is represented by the first ordination axis, which, like the first ordination axis of the Grusha Ozero record, primarily reflects variation in the abundance of the two dominant taxa *S. pinnata* (r = 0.92, $p \ll 0.001$) and *S. elliptica* (r = 0.84, $p \ll 0.001$). The second ordination axis primary reflects variation in *S. construens* and to a lesser extent *P. brevistriata*, while the third axis is positively correlated (r = 0.7, $p \ll 0.001$) to the Shannon diversity index.

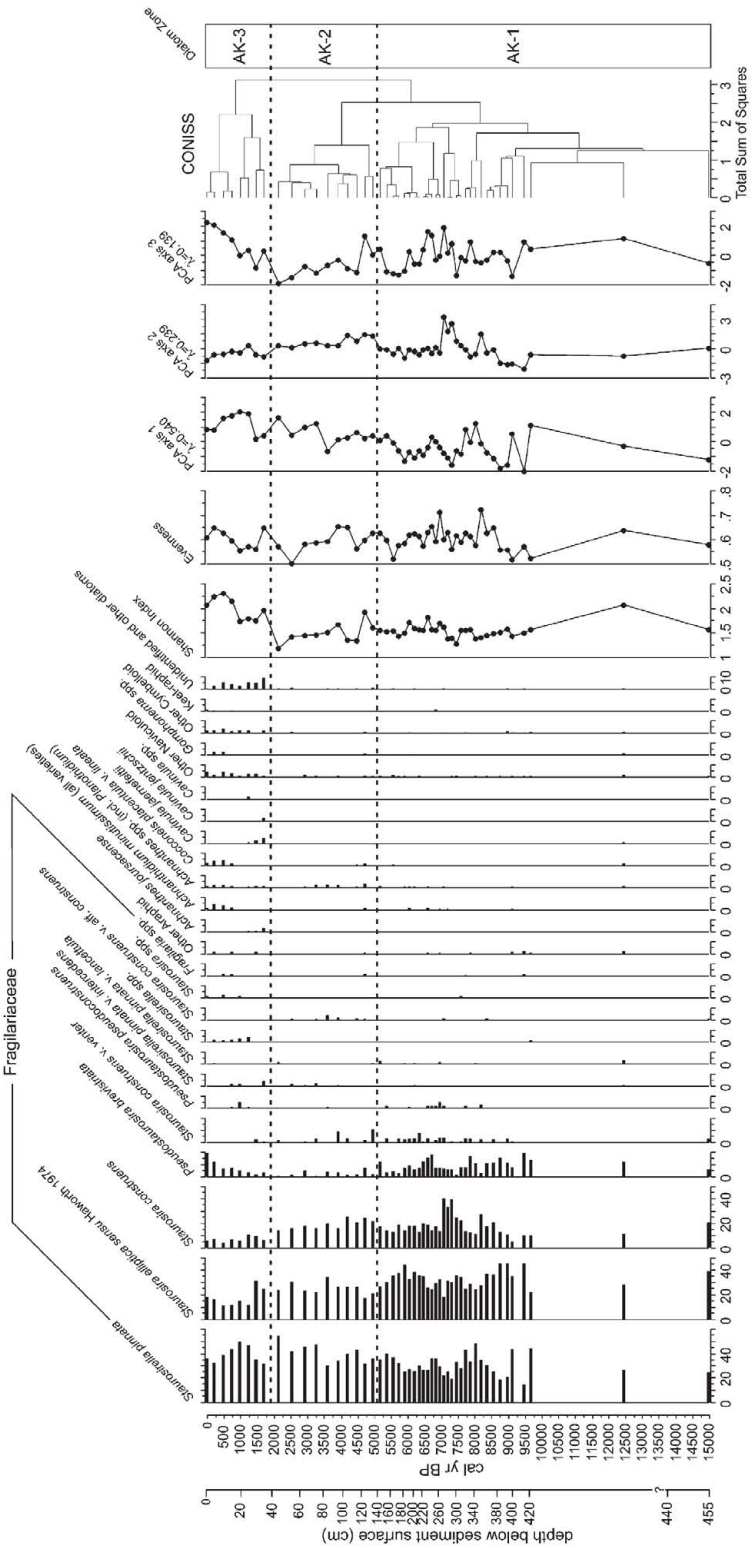

Figure 8. Akkol Diatom Stratigraphy. Species with relative abundances greater than 2% are plotted, as are the Shannon and Evenness indices of diversity and the sample scores for the first three PCA axes. Zonation is based on the CONISS algorithm with significant clusters identified by the broken-stick model.

Discussion

The diatom records of Dzhangyskol, Grusha Ozero, and Akkol are broadly similar in terms of community structure and dominant taxa. Throughout their histories, all three lakes have lacked a significant planktonic community and have been dominated by small benthic alkaliphilic species of the Fragilariaceae family commonly found in alpine (Lotter et al. 1997; Karst-Riddoch et al. 2005) and arctic lakes (Douglas and Smol 1999; Laing and Smol 2000). The dominance of these taxa may be related to the high surface-to-volume ratio of small cells coupled with higher specific growth rates, which may confer a competitive advantage to small taxa under low nutrient conditions (Lotter et al. 1999). Furthermore, these taxa inhabit the littoral zone, which is the first area to become ice-free. Thus, these taxa may quickly form blooms and outcompete larger and/or planktonic diatoms during the short growing season (Smol 1988; Lotter et al. 1999). However, these taxa also can dominate emergent coastal lakes (Stabell 1985), shallow, nutrient-rich lakes (Bennion et al. 2001), and late-glacial pioneer assemblages (Haworth 1976). Given the wide range of environments in which these taxa have been found, Anderson (2000) suggests that light and tolerance of physical disturbance may be the most important factors controlling their distribution.

The dominance of *Staurosira*, *Staurosirella*, and *Pseudostaurosira* species has made direct paleolimnological interpretations difficult, as our present understanding of diatom ecology lacks the detail necessary to interpret variation in species relative abundance among these taxa. At present, we lack a regional calibration set. A calibration dataset from the Alps is restricted to humid and sub-humid climates, making its extension to the more continental mountain ranges of Eurasia questionable. The mountains of southern Siberia feature high-elevation steppe landscapes, an environment in which the diatom distribution is unknown. Furthermore, these species' apparently wide ecological tolerances, especially with respect to nutrients, tend to reduce their predictive power (Bennion et al. 2001).

Although we lack information with which to draw climatic or environmental inferences directly from the diatom record, additional proxy data provide insight into the source of diatom assemblage variability. The diatom record of Grusha Ozero is characterized by large alternations in the relative abundance of *S. pinnata* and *S. elliptica*. The relative abundance of *S. pinnata* is significantly correlated ($r = 0.84$, $p \ll 0.001$) with the first DCA axis of the chironomid record (Ilyashuk and Ilyashuk, unpublished data) of Grusha Ozero (Figure 9). This ordination axis of the chironomid record is interpreted as a temperature gradient and implies an association between high abundance of *S. pinnata* and cold temperatures. Conversely, *S. elliptica* corresponds to warmer temperatures. This association is consistent with the observations of Laing and Smol (2000) of the modern distribution of diatoms in lakes in three regions of Arctic Siberia. They found the highest abundances of *S. pinnata* in tundra lakes in all regions, while abundances in taiga lakes were usually less than 20%. The distribution of *S. construens* v. *venter*, which is probably conspecific with the taxon we have identified as *S. elliptica*, is more complex. In the western and central regions, *S. construens* v. *venter* was abundant in all zones. However, in the eastern region, this taxon was found in highest abundance in the taiga zone, although at less than 20% abundance.

At Grusha Ozero, the oldest pollen assemblage zone, which correlates with diatom zone GR-1, is dominated by herbaceous taxa (*Artemisia*, Poaceae, Cyperaceae, and Chenopodiaceae) similar to that of modern tundra–steppe plant communities described in the southeastern Altai (Blyakharchuk, unpublished data). After 11,900 cal year BP (195 cm), the pollen record indicates the decline of alpine meadow and development of a steppe-shrubland. This assemblage is absent from Akkol, which coupled with the radiocarbon results, suggests that the lake may have been dry at this time. The first appearance of the aquatic plant *Myriophyllum verticillatum* in Grusha Ozero also occurs during this period, corresponding to an interval of fibrous sediment. A more complex habitat associated with the presence of aquatic macrophytes could explain the high diversity of diatoms observed in GR-2. Arboreal pollen, particularly *Pinus sibirica* but also *Picea obovata*, *Abies sibirica*, and *Larix sibirica*, dominates between ~10,400 and 5,900 cal year BP (140–45 cm). The beginning of this pollen

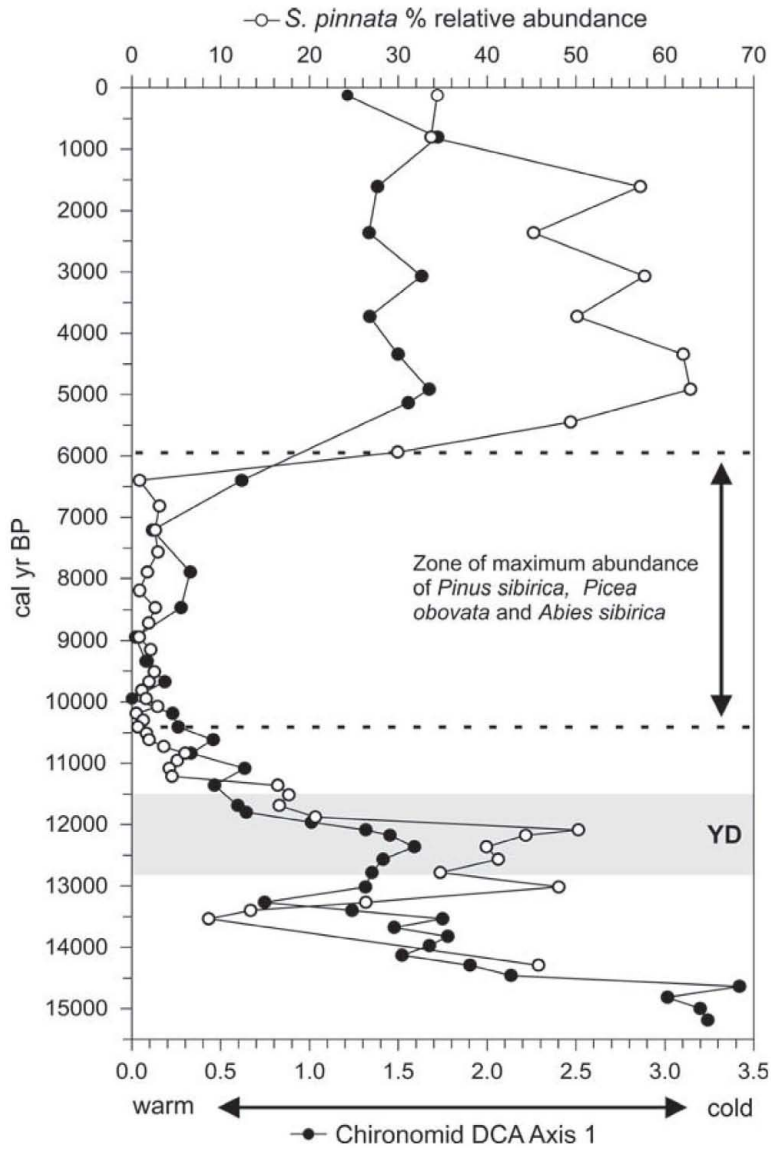

Figure 9. Correlation ($r = 0.84$, $p \ll 0.001$) between chironomid and diatom sedimentary records of Grusha Ozero. The first DCA axis of the chironomid record (Ilyashuk and Ilyashuk, unpublished data) is interpreted as a temperature gradient. The relative abundance of the diatom taxon *S. pinnata* decreases significantly during the inferred warm interval from ~11,200 to 6,000 cal year BP. The chironomid-inferred warm interval correlates with pollen evidence of increased *Pinus sibirica*, *Picea obovata*, and *Abies sibirica*, implying a warmer and more humid climate. A cooling oscillation between ~13,300 and 11,900 cal year BP interrupted late-glacial warming. Given uncertainties in our chronology, this event may correspond to the Younger Dryas Stade denoted by the shaded box.

zone slightly lags the period of warm temperatures inferred from the chironomid record and the decline of *S. pinnata* (Figure 9). However, uncertainty in the age model during this interval precludes accurate estimation of the length of time represented by the lag. LOI_{550} nearly doubles to 40% between ~12,100 and 11,700 cal year BP (200 and 190 cm), coinciding with the decline in *S. pinnata* and chironomid-inferred warming trend. Peak organic productivity, which occurs between 8,900 and 6,400 cal year BP (90 and 50 cm) (Figure 4b), coincides with maximal abundance of *Pinus sibirica*. After ~5,900 cal year BP (45 cm), an increase in *S. pinnata* and chironomid-inferred cooling correspond to decreased arboreal pollen (*P. sibirica, P. obovata*, *A. sibirica*, and *L. sibirica*) and increased *Artemisia* and Poaceae.

Despite their close proximity, the diatom records of Grusha Ozero and Akkol do not show a close correspondence. The low variability in the diatom record of Akkol implies a lack of sensitivity of the diatom community to climate and/or climate-mediated changes in the catchment and lake. Here, diatoms reveal a similar but much weaker relationship with chironomids than that observed at Grusha Ozero. The relative abundance of *S. pinnata* averaged 31% between ~9,700 and 5,200 cal year BP (425–145 cm) and increased to 40% after 5,200 cal year BP. Conversely, *S. elliptica* relative abundance averaged 33% prior to 5,200 cal year BP, but only 22% after that date. The chironomid record of Akkol suggests maximum warmth between ~8,200 and 6,200 cal year BP (355–205 cm) (Ilyashuk and Ilyashuk, unpublished data). The boundary between zones AK-1 and AK-2 at ~5,200 cal year BP (145 cm) corresponds approximately to increases in herbaceous pollen at Akkol (Blyakharchuk, unpublished data). The differential response of otherwise similar diatom communities at Grusha and Akkol may be related to lake processes influenced by morphometry and landscape position.

Although diatom community composition shows little change, the record of BSi accumulation suggests that diatom productivity at Akkol has responded to millennial scale variability in climate driven by changes in insolation. Productivity in arctic and alpine lakes is particularly sensitive to climate as a consequence of short growing seasons. Warmer spring and summer temperatures induce earlier ice-off, with the result that a larger proportion of the lake is available for photosynthetic growth for a longer period of time (Smol 1988; Wolfe 2003). Furthermore, increased summer temperature may be linked to enhanced export of nutrients from catchment to lake (Wolfe 2003). Figure 7 compares BSi flux to changes in July insolation at 50N over the past 10,000 years. From ~7,900 cal year BP (335 cm) to present, BSi accumulation rates show a gradual declining trend that corresponds to the decrease in insolation. The discrepancy between BSi accumulation rates and the insolation curve before 8,000 cal year BP may be related to high flux of minerogenic material, which is reflected in an LOI550 of less than 8% until ~8400 cal year BP (365 cm). Aridity and related low water levels during the early-Holocene also may have reduced habitat availability and nutrient export. Sub-millennial variations in BSi accumulation rates superimposed on the long-term decreasing trend cannot be linked to higher-frequency variations in climate or solar forcing at this time.

Diatoms are largely absent from late-glacial sediments of Dzhangyskol, which at the time was a meltwater lake formed by advance of the Kurumundu glacier. Extended ice-cover (Smol 1988) and/or high rates of minerogenic sediment flux (Anderson 2000) may have inhibited development of a diatom community during this period. After ~11,800 cal year BP (308 cm), organic matter increased (Figure 4a) as the surrounding landscape was vegetated and diatoms increased in abundance. Warm summers eventually led to failure of the ice dam and partial draining of the lake. An *Artemisia* steppe is inferred from the pollen record, and increases in pollen and spores of aquatic plants suggest warmer water. Increased diatom diversity and the abundance of non-Fragilariaceae epiphytic taxa in this zone are consistent with increasing habitat complexity in the aquatic environment and soil development in the catchment.

Increased moisture in the early-Holocene promoted a gradual transition from steppe to forest. The corresponding diatom assemblage is characterized by relatively low diversity with few non-Fragilariaceae taxa. Warm-water vegetation present in lacustrine sediment of the pingos suggests that Dzhangyskol did not freeze completely during winter (Butvilovsky 1993). An unconformity indicates draining of Dzhangyskol at the site of the core at ~7,500 cal year BP, probably caused by diversion of its inflowing meltwater stream. The lake refilled and deposition resumed by ~5,500 cal year BP. A shift in $\delta^{18}O$ of bio-induced carbonate from –17 to –9‰ (Wright and Ito, unpublished data) coinciding with the unconformity, implies a shift from a primary glacial meltwater source to a local precipitation source. The diatom community shows no response to this change in water source or size of the lake.

After 6,500 cal year BP forests of *Pinus sibirica* and *Larix siberica* expanded to replace more mesophilous *Abies* and *Picea* species, while steppe communities spread in the dry intermontane basins and south-facing slopes. *Staurosirella pinnata*, the taxon

associated with cooler temperatures in the Grusha Ozero record, increased in abundance after ~5,000 cal year BP (112 cm). The development of pingos and expansion of permafrost after ~2,100 cal year BP coincide approximately with the onset of DZH-2.

Grusha Ozero provides the oldest and most complete record of late-glacial climatic and ecological change. The chironomid and diatom records (Figure 9) suggest initial warming of climate after ~14,300 cal year BP, interrupted by a return to cooler temperatures between ~13,300 and 11,900 cal year BP (222 and 195 cm). This period is also characterized by a decrease in organic matter (Figure 4b). The increase in organic matter at the end of this interval, which signals increased terrestrial and aquatic productivity, is a common feature of the Younger Dryas/Holocene boundary. This climatic oscillation is not evident in the pollen record. Although our chronology indicates this event slightly predates the Younger Dryas Stade (~12,800–11,500 cal year BP; Alley 2000), uncertainty in our age model is large enough that this event may be contemporaneous with the Younger Dryas Stade. After ~12,000 cal year BP, continued aridity is inferred from the dominance of *Artemisia* steppe and the possible drying of Akkol.

By 10,400 cal year BP (140 cm) chironomids, diatoms, and pollen suggest climatic warming that is consistent with upslope movement of altitudinal vegetation belts reported from a site north of the Karaginskaya Basin (Ponomareva et al. 1991; Butvilovsky 1993) and development of closed forests with *Picea* and *Abies* in the central Altai (Blyakharchuk et al. 2004). The expansion of forest into the interior ranges, where moisture is presently limiting, also indicates increased humidity. The period between ~8,200 and 6,500 cal year BP is inferred to be the warmest and most humid, based on the maximum occurrence of *A. sibirica* (the most thermophilous tree among Siberian species) and is consistent with maximum diatom productivity at Akkol. However, there is no response in diatom community composition to these inferred changes in effective moisture.

Deforestation after ~6,000 cal year BP is consistent with chironomid and diatom evidence of cooling. In the Karaginskaya basin, the disappearance of dark-coniferous forests and expansion of steppe and herbaceous alpine taxa suggest colder and drier conditions. These changes coincide with the expansion of the more continental *Pinus* and *Larix* and decline of *Picea* and *Abies* in the western Altai (Blyakharchuk et al. 2004).

The response of the diatom communities in these lakes to warming and forest expansion differs from changes reported in other Eurasian paleolimnological studies (Laing et al. 1999; Lotter and Bigler 2000) and modern calibration studies (Lotter et al. 1997; Laing and Smol 2000) that span arctic and alpine treeline. One reported response to increased temperatures has been an increase in planktonic taxa, associated with longer growing seasons, altered thermal regimes, changes in transparency, and/or nutrient availability. The shallow depths of our study lakes may have precluded these lakes from exhibiting such a response. With respect to changes in benthic taxa associated with changes in alkalinity, DOC, and/or nutrients caused by vegetation change, it is possible, in the cases of Grusha Ozero and Akkol, that their catchments were never forested. The elevated percentage of arboreal pollen could simply reflect the advance of the forest limit, which is currently 40 km to the west of the study sites, sufficiently close to contribute pollen to the watersheds. The lack of a diatom response to the shift from steppe to forested catchment at Dzhangyskol during the early-Holocene may reflect the contribution of glacial meltwater via the Kurkurek River. However, the lack of a response of the diatoms following the isotope-inferred diversion of this river seems inconsistent with this explanation. Perhaps frequent disturbance and cooling temperatures favored Fragilariaceae taxa after resumption of sedimentation.

Although the diatom floras of the three study lakes are quite similar, clear differences exist in the magnitude of stratigraphic variation of the diatom assemblages, and by inference the sensitivity of the lakes to environmental variability. Grusha Ozero and Dzhangyskol feature the most variability, although it is manifested among different parts of the diatom community. Grusha Ozero experienced abrupt fluctuations in the abundance of its dominant Fragilariaceae taxa, while more of Dzhangyskol's variation was related to changes in the abundance of its sub-dominant and rare taxa. The apparent long-term turnover of the subdominant and rare taxa may reflect long-term soil and vegetation development in

the catchment, which could be expected to influence nutrient and DOC exports to the lake. In addition, Dzhangyskol, which is situated at a lower elevation and within a more humid zone, is characterized by a numerically richer flora than the steppe lakes. Both Dzhangyskol and Akkol show increasing trends in diatom diversity beginning at ~2,000 cal year BP and peaking in the past 750 years.

Conclusions

From the late-glacial to the present, the diatom floras of Dzhangyskol, Grusha Ozero, and Akkol have been dominated by small Fragilariaceae taxa. These ecological generalists are common in lakes at high elevations and high latitudes, where ice-free intervals are short and nutrient supply is low, although they occur across a wide ecological gradient. Dzhangyskol, the only lake presently located in a forested catchment, has the richest flora and has experienced long-term turnover of its subdominant and rare taxa.

Direct paleoenvironmental interpretations from the diatom record are limited by the apparent complexity of environmental drivers and a lack of information on the ecological affinities of the dominant taxa. The diatom record of Grusha Ozero, located within the high-elevation Karaginskaya basin, is characterized by abrupt shifts in dominance between *S. elliptica* and *S. pinnata*, in addition to more subtle changes in the composition of its subdominant taxa. Based on chironomid analysis of the same core, variability in the relative abundance of *S. pinnata* appears to reflect millennial-scale fluctuations in temperature. Akkol, also located in the Karaginskaya basin, has shown significantly less variability in the composition of its diatom community through time, although the last 2,000 years have featured increased diversity. However, diatom productivity, inferred from accumulation rates of biogenic silica, appears to track declining insolation over the past 8,000 years. A more refined understanding of the proximate control on diatom distribution, particularly in freshwater lakes of the interior steppe, is required to fully explain the major components of stratigraphic variation of the diatom record in the Altai lakes investigated.

Late-glacial and Holocene millennial-scale climatic variability is inferred from synthesis of all available proxies (diatoms, chironomids, pollen, BSi, and LOI). Cooling that is probably correlative to the Younger Dryas Stade is detected. The early-Holocene was characterized by a warmer and more humid climate that resulted in afforestation of steppe landscapes. Temperature and humidity began to wane by ~6,000 cal year BP, and the modern biomes became established.

Acknowledgments

This research was supported by grants to H. E. Wright and S. C. Fritz from the National Science Foundation and the National Geographic Society. Pavel Blyakharchuk, Pavel Borodavko, and Brigitta Ammann assisted with collection of the sediment cores analyzed in this study. Boris Ilyashuk and Elena Ilyashuk generously shared the results of their chironomid analysis of Grusha Ozero and Akkol. Florencia Oberli analyzed the sediments for LOI at the University of Bern.

References

Alley R.B. 2000. The Younger Dryas cold interval as viewed from central Greenland. Quat. Sci. Rev. 19: 213–226.

Anderson N.J. 2000. Diatoms, temperature and climatic change. Eur. J. Phycol. 35: 307–314.

Andreev A.A., Siegert C., Klimanov V.A., Derevyagin A.Y., Shilova G.N., and Melles M. 2002. Late Pleistocene and Holocene vegetation and climate on the Taymyr Lowland, Northern Siberia. Quat. Res. 57: 138–150.

Beniston M., Diaz H.F. and Bradley R.S. 1997. Climatic change at high elevation sites: an overview. Climatic Change 36: 233–251.

Bennett K.D. 1996. Determination of the number of zones in a biostratigraphical sequence. New Phytol. 132: 155–170.

Bennett K.D. 2002. Documentation for psimpoll 4.10 and pscomb 1.03. http://www.kv.geo.uu.se/psimpoll.html

Bennion H., Appleby P.G., and Phillips G.L. 2001. Reconstructing nutrient histories in the Norfolk Broads, UK: implications for the role of diatom-total phosphorus transfer functions in shallow lake management. J. Paleolimnol. 26: 181–204.

Berger A. and Loutre M.F. 1991. Insolation values for the climate of the last 10 million years. Quat. Sci. Rev. 10: 297–317.

Blyakharchuk T.A. 2003. Four new pollen sections tracing the Holocene vegetational development of the southern part of the West Siberian Lowland. The Holocene 13: 715–731.

Blyakharchuk T.A. and Sulerzhitskiy L.D. 1999. Holocene vegetational and climatic changes in the forest zone

of Western Siberia according to pollen records from the extrazonal palsa bog Bugristoye. The Holocene 9: 621–628.

Blyakharchuk T.A., Wright H.E., Borodavko P.S., van der Knaap W.O., and Ammann B. 2004. Late-glacial and Holocene vegetational changes on the Ulagan high-mountain plateau, Altai Mountains, southern Siberia. Paleogeogr. Paleoclimatol. Paleoecol. 209: 259–279.

Borisov A.A. 1965. Climates of the U.S.S.R. Aldine Pub. Co, Chicago, 255 pp.

Butvilovsky V.V. 1993. Paleogeografiya poslednego oledeneniya i Golotsena Altaya: sobytiino-katastroficheskaya model' (Palaeogeography of the last glaciation and Holocene of Altai: event–catastrophic model). Tomsk State University Press, Tomsk, 252 pp. (in Russian)

Camburn K.E. and Charles D.F. 2000. Diatoms of Low-alkalinity Lakes in the Northeastern United States. The Academy of Natural Sciences of Philadelphia, Philadelphia, 152 pp.

Conley D.J. 1998. An interlaboratory comparison for the measurement of biogenic silica in sediments. Mar. Chem. 63: 39–48.

Conley D.J. and Schelske C.L. 2001. Biogenic silica. In: Smol J.P., Birks H.J.B., and Last W.M. (eds), Tracking Environmental Change Using Lake Sediments Volume 3: Terrestrial, Algal, and Siliceous Indicators. Kluwer, Dordrecht, pp. 281–293.

Davydova N.N., Subetto D.A., Khomutova V.I., and Sapelko T.V. 2001. Late Pleistocene–Holocene paleolimnology of three northwestern Russian lakes. J. Paleolimnol. 26: 37–51.

DeMaster D.J. 1979. The marine budgets of silica and ^{32}Si. Ph.D. Dissertation, Yale University, 308 pp.

Douglas M.S.V. and Smol J.P. 1999. Freshwater diatoms as indicators of environmental change in the High Arctic. In: Stoermer E.F. and Smol J.P. (eds), The Diatoms: Applications for the Environmental and Earth Sciences. Cambridge University Press, Cambridge, pp. 227–244.

Fallu M.-A., Allaire N., and Pienitz R. 2000. Freshwater diatoms from northern Québec and Labrador (Canada). Bibliotheca Diatomologica Band 45. J. Cramer, Berlin, 200 pp.

Fowell S.J., Hansen B.C.S., Peck J.A., Khosbayar P., and Ganbold E. 2003. Mid to late Holocene climate evolution of the Lake Telmen Basin, North Central Mongolia, based on palynological data. Quat. Res. 59: 353–363.

Glebov F.Z., Karpenko L.V., and Dahkovskaya I.S. 2002. Climatic changes, successions of peatlands and zonal vegetation, and peat accumulation dynamics in the Holocene (the West-Siberia peat profile "Vodorasdel." Climatic Change 55: 175–181.

Groisman P. 1998. Former Soviet Union Monthly Precipitation Archive, 1891–1993. Data provided by the EOS Distributed Active Archive Center (DAAC) at the National Snow and Ice Data Center. University of Colorado, Boulder, CO.

Harrison S.P., Prentice I.C., and Bartlein P.J. 1992. Influence of insolation and glaciation on atmospheric circulation in the North Atlantic sector: implications of General Circulation Model experiments for the late Quaternary of Europe. Quat. Sci. Rev. 11: 283–299.

Harrison S.P., Yu G., and Tarasov P.E. 1996. Late Quaternary lake-level record from northern Eurasia. Quat. Res. 45: 138–159.

Haworth E.Y. 1974. A scanning electron microscope study of some different frustule forms of the genus *Fragilaria* found in Scottish late-glacial sediments. Br. Phycol. J. 10: 73–80.

Haworth E.Y. 1976. Two late-glacial (Late Devensian) diatom assemblage profiles from northern Scotland. New Phytol. 77: 227–256.

Heiri O., Lotter A.F., and Lemcke G. 2001. Loss-on-ignition as a method for estimating organic and carbonate content in sediments: reproducibility and comparability of results. J. Paleolimnol. 25: 101–110.

Karst-Riddoch T.L., Pisaric M.F.J., and Smol J.P. 2005. Diatom responses to 20th century climate-related environmental changes in high-elevation mountain lakes of the northern Canadian Cordillera. J. Paleolimnol. 33: 265–282.

Khotinskiy N.A. 1984. Holocene vegetation history. In: Velichko A.A., Wright H.E. Jr., and Barnosky C.W. (eds), Late Quaternary Environments of the Soviet Union. University of Minnesota Press, Minneapolis, pp. 179–200.

Koropachinsky I.Y. 1996. Green Book of Siberia: Rare and Endangered Plant Communities. Nauka (Russian Academy of Sciences, Novosibirsk, 396 pp (in Russian).

Krammer K. and Lange-Bertalot H. 1986–1991. Bacillariophyceae. In: Ettl H., Gerloff J., Heynig H., and Mollenhauser D. (eds), Süßwasserflora von Mitteleuropa Band 2(1–4). Gustav Fisher Verlag, Stuttgrat/Jena.

Kremenetski K.V., Velichko A.A., Borisova O.K., MacDonald G.M., Smith L.C., Frey K.E., and Orlova L.A. 2003. Peat-lands of the Western Siberian lowlands: current knowledge on zonation, carbon content and Late Quaternary history. Quat. Sci. Rev. 22: 703–723.

Kultti S., Väliranta M., Sarmaja-Korjonen K., Solovieva N., Virtanen T., Kauppila T., and Eronen M. 2003. Palaecological evidence of changes in vegetation and climate during the Holocene in the pre-Polar Urals, northeast European Russia. J. Quat. Sci. 18: 503–520.

Laing T.E., Rühland K.M., and Smol J.P. 1999. Past environmental and climatic changes related to tree-line shifts inferred from fossil diatoms from a lake near the Lena River Delta, Siberia. Holocene 9: 547–557.

Laing T.E. and Smol J.P. 2000. Factors influencing diatom distributions in circumpolar treeline lakes of northern Russia. J. Phycol. 36: 1035–1048.

Lange-Bertalot H. and Metzelin D. 1996. Indicators of Oligotrophy. Iconogr. Diatomol. Vol. 2, 390 pp.

Lepš J. and Šmilauer P. 2003. Multivariate Analysis of Ecological Data using CANOCO. Cambridge University Press, Cambridge, UK, 269 pp.

Lotter A.F. and Bigler C. 2000. Do diatoms in the Swiss Alps reflect the length of ice-cover? Aquat. Sci. 62: 125–141.

Lotter A.F., Birks H.J.B., Hofmann W., and Marchetto A. 1997. Modern diatom, cladocera, chironomid, and chrysophyte cyst assemblages as quantitative indicators for the reconstruction of past environmental conditions in the Alps. I. Climate. J. Paleolimnol. 18: 395–420.

Lotter A.F., Pienitz R., and Schmidt R. 1999. Diatoms as indicators of environmental change near arctic and alpine treeline. In: Stoermer E.F. and Smol J.P. (eds), The Diatoms: Applications for the Environmental and Earth Sciences. Cambridge University Press, Cambridge, pp. 205–226.

Lydolph P.E. 1977. Climates of the Soviet Union (World Survey of Climatology 7). Elsevier Scientific Publishing, Amsterdam, 441 pp.

MacDonald G.M., Velichko A.A., Kremenetski C.V., Borisova O.K., Goleva A.A., Andreev A.A., Cwynar L.C., Riding R.T., Forman S.L., Edwards T.W.D., Aravena R., Hammarlund D., Szeicz J.M., and Gattaulin V.N. 2000. Holocene treeline history and climate change across northern Eurasia. Quat. Res. 53: 302–311.

Malyshev L. and Nimis P.L. 1997. Climatic dependence of the ecotone between alpine and forest orobiomes in southern Siberia. Flora 192: 109–120.

Overpeck J.T., Webb T. III, and Prentice I.C. 1985. Quantitative interpretation of fossil pollen spectra: dissimilarity coefficients and the method of modern analogs. Quat. Res. 23: 87–108.

Peck J.A., Khosbayar P., Fowell S.J., Pearce R.B., Ariunbileg S., Hansen B.C.S., and Soninkhishig N. 2002. Mid to Late Holocene climate change in north central Mongolia as recorded in the sediments of Lake Telmen. Paleogeogr. Paleoclimatol. Paleoecol. 183: 135–153.

Peteet D., Andreev A., Bardeen W., and Mistretta F. 1998. Long-term Artic peatland dynamics, vegetation, and climate history of the Pur-Taz region, Western Siberia. Boreas 27: 115–126.

Pisaric M.F.J., MacDonald G.M., Velichko A.A., and Cwynar L.C. 2001. The Lateglacial and Postglacial vegetation history of the northwestern limits of Beringia, based on pollen, stomate and tree stump evidence. Quat. Sci. Rev. 20: 235–245.

Ponomareva E.A., Butvilovsky V.B., and Orlova L.A. 1991. Section Bogoyash—basic Holocene section of the high mountain belt of southeastern Altai. In: Baryshnikov G. Ya. (ed.), Novye dannye po geologicheskomy stroeniyu i usloviyam formirovaniya mestorozhdenii poleznukh iskopaemykh v Altaiskom krae. Altai State University, Barnaul.

Porinchu D.F. and Cwynar L.C. 2002. Late-Quaternary history of midge communities and climate from a tundra site near the lower Lena River, Northeast Siberia. J. Paleolimnol. 27: 59–69.

Smol J.P. 1988. Paleoclimate proxy data from freshwater arctic diatoms. Verh. Int. Ver. Limnol. 23: 837–844.

Stabell B. 1985. The development and succession of taxa within the diatom genus *Fragilaria* Lyngbye as a response to basin isolation from the sea. Boreas 14: 273–286.

Stuiver M. and Reimer P.J. 1993. Extended ^{14}C database and revised CALIB radiocarbon calibration program. Radiocarbon 35: 215–230.

Stuiver M., Reimer P.J., and Braziunas T.F. 1998a. High-precision radiocarbon age calibration for terrestrial and marine samples. Radiocarbon 40: 1127–1151.

Stuiver M., Reimer P.J., Bard E., Beck J.W., Burr G.S., Hughen K.A., Kromer B., McCormac F.G., v. d. Plicht J., and Spurk M. 1998b. INTCAL98 Radiocarbon age calibration 24,000–0 cal BP. Radiocarbon 40: 1041–1083.

Tarasov P., Dorofeyuk N., and Metel'tseva E.V. 2000. Holocene vegetation and climate changes in Hoton-Nur basin, northwest Mongolia. Boreas 29: 117–126.

Tarasov P.E., Guiot J., Cheddadi R., Andreev A.A., Bezusko L.G., Blyakharchuk T.A., Dorofeyuk N.I., Filimonova L.V., Volkova V.S., and Zernitskaya V.P. 1999. Climate in northern Eurasia 6000 years ago reconstructed from pollen data. Earth Planet. Sci. Lett. 171: 635–645.

ter Braak C.J.F. and Šmilauer P. 1998. CANOCO reference manual and user's guide to Canoco for Windows: software for canonical community ordination (version 4). Microcomputer Power, Ithaca, New York, 352 pp.

Väliranta M., Kaakinen A., and Kuhry P. 2003. Holocene climate and landscape evolution east of the Pechora Delta, East-European Russian Arctic. Quat. Res. 59: 335–344.

Williams D.M. and Round F.E. 1987. Revision of the genus *Fragilaria*. Diatom Res. 2: 267–288.

Wolfe B.B., Edwards T.W.D., Aravena R., Forman S.L., Warner B.G., Velichko A.A., and MacDonald G.M. 2000. Holocene paleohydrology and paleoclimate at treeline, north-central Russia, inferred from oxygen isotope records in lake sediment cellulose. Quat. Res. 53: 319–329.

Wolfe A.P. 2003. Diatom community responses to late-Holocene climatic variability, Baffin Island, Canada: a comparison of numerical approaches. Holocene 13: 29–37.

WWF Climate Program. 2001. Climate Passport of the Altai-Sayan Ecoregion. World Wildlife Foundation, Moscow, 26 pp.

Wright H.E. Jr. 1991. Coring tips. J. Paleolimnol. 6: 37–49.

Yu G. and Harrison S.P. 1995. Holocene changes in atmospheric circulation patterns as shown by lake status changes in northern Europe. Boreas 24: 260–268.